

High Performance and Reliable Torque Control of Permanent Magnet Synchronous Motors in Electric Vehicle Applications

V. Erginer¹, M. H. Sarul¹

¹*Department of Electrical Engineering, Yildiz Technical University, Esenler, Istanbul, Turkey
volkanerginer@tmail.com*

Abstract—This paper presents a novel, high performance maximum torque per ampere control (MTPAC) of an interior permanent magnet synchronous motor (IPMSM) that is chosen for a vehicular application. In vehicular applications IPMSMs are usually controlled with MTPAC method due to fully utilization of reluctance torque, usually with this method maximum torque per ampere trajectories are obtained by look up tables because of nonlinear relation between torque and current; however, utilization of look up tables decreases the real time performance and reliability of the system. Some studies have been used MTPAC with nonlinear equations between d-q axes currents and torque; however, controller calculation burden can be reduced with proposed method. In this study relationship between torque and stator current magnitude is obtained as a first order linear equation with curve fitting. Thereby it has been possible to work with only one linear torque equation instead of nonlinear equations, therefore controller performance and reliability is increased. Control of the motor is simulated under different load conditions, and results are given and analysed.

Index Terms—Electric vehicles, permanent magnet, motors.

I. INTRODUCTION

Interior permanent magnet synchronous motors (IPMSM) are widely used in modern drive applications. Electric vehicle is one of the most important areas for IPMSM technology due to its high power/weight ratio [1]. Achieving maximum torque/ampere ratio is a critical issue especially in constant torque region. Some vector control methods use only q axis stator current (i_{qs}), which is proportional to torque (T_e), in constant torque region, and d axis current (i_{ds}) remains zero [2], [3]. However, it obstructs the usage of reluctance torque. On the other hand, there are several approaches to make use of reluctance torque like unity power factor control [4], maximum efficiency control [5] and maximum torque per ampere control [6]–[11]. However, none of these works dealt with calculation complexity of the controller, only in [6] a curve fitting method proposed, however it is possible to obtain a simpler and accurate current-torque relation.

Maximum Torque per Ampere Control (MTPAC) is an effective choice for vehicular applications due to fully

utilization of reluctance torque. The relationships between torque and stator current components in MTPAC of IPMSMs are complex and difficult to solve, and they reduce the performance of control systems. Usually look up tables are used to solve this problem. However, working with look up tables increases the calculation burden of control system and it affects negatively real time performance and reliability [6].

In this study a novel method with MTPAC of an IPMSM is simulated for a vehicular application. The relationship between i_s and T_e is obtained with curve fitting, and thus it is achieved to represent relationship of stator current components vs. torque with a first order linear equation that gives coherent results in accordance with IPMSM model via a simple correlation; consequently, real time performance of the control system is improved via calculation of stator current components with these simple equations. The effectiveness of proposed method is denoted with simulation results.

II. INTERIOR PERMANENT MAGNET SYNCHRONOUS MOTORS AS TRACTION MOTORS

Different types of motors are used in electric vehicles in the market. A brief comparison can be seen in Table I [12]–[14].

TABLE I. COMPARISON OF MOTOR TYPES.

	Benefits	Drawbacks
DC MOTOR	Linear Torque-Current Relation	Low Reliability
	Low Torque Ripple	Maintenance Requirement
	Simple Control	Low Torque/Volume Ratio
INDUCTION MOTOR	Low Price	Lagging Power Factor
	Simple Construction	Complicated Control
		Medium Efficiency
IPMSM	High Efficiency	Expensive
	High Torque/Volume Ratio	Danger of Demagnetization of the Magnets
	Good Overloading Capacity	

IPMSM's interior permanent magnets in rotor are a favorite for vehicular applications due to their mechanical integrity and stronger armature reaction. IPMSM cross section can be seen in Fig. 1 and phasor diagram can be seen

in Fig. 2. [15], [16]

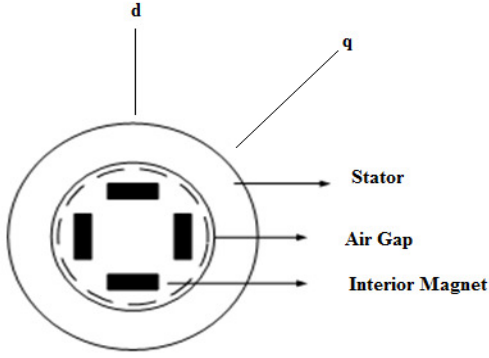


Fig. 1. Cross section of IPMSM.

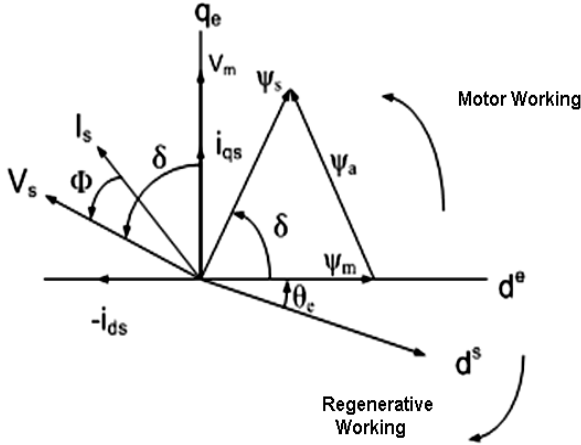


Fig. 2. Phasor diagram of IPMSM.

When the motor rotates forward, phasor diagram rotates with ω_e synchronous speed in counterclockwise to d^s axis. The angle between d^e magnet axis and d^s is always defined as $\theta_e = \omega_e t$. Armature reaction flux phasor (ψ_a) is defined below:

$$\psi_a = \frac{\hat{\psi}_a}{\sqrt{2}} = \frac{1}{\sqrt{2}} \sqrt{\psi_{ds}^2 + \psi_{qs}^2}, \quad (1)$$

$$\psi_a = \frac{1}{\sqrt{2}} \sqrt{(L_{ds} i_{ds})^2 + (L_{qs} i_{qs})^2}. \quad (2)$$

Sum of armature reaction flux ψ_a and magnet flux ψ_m gives stator flux ψ_s which has δ angle with d^e axis. Stator phase voltage V_s and induced emf V_m are defined respectively as $\omega_e \psi_s$ and $\omega_e \psi_m$, and these fluxes are perpendicular to the voltages that produce these fluxes. Due to high inductance values of IPMSM its armature reaction flux is higher than surface mounted permanent magnet motor's as can be seen from (1) and (2). Additionally, this feature provides to operate in a wider speed range in field weakening region.

Different control methods can be implemented for IPMSMs that used in electric vehicles. In these control methods MTPAC is the most impressive one.

III. MAXIMUM TORQUE PER AMPERE CONTROL

IPMSM is a convenient motor to operate in high speeds due to its mechanical integrity, and strong armature reaction

effect enables to operate in a wide speed range in field weakening region. Because of these reasons interior magnet rotor construction is more appropriate for traction motors than surface mounted magnet rotor construction. IPMSM has saliency and its d-q axes inductance values are not the same as can be seen in (3) and (4):

$$L_{ds} = L_{dm} + L_{ls}, \quad (3)$$

$$L_{qs} = L_{qm} + L_{ls}, \quad (4)$$

when $L_{dm} \neq L_{qm}$.

On the other hand, leakage inductances are not affected by rotor construction and they are equal to each other.

Excitation current (I_m) is accepted constant in motor's steady state analyse, thus air gap flux ($\psi_m = L_m I_m$) is also becomes constant. On the other hand, transient equivalent circuits are defined on rotating axis frame.

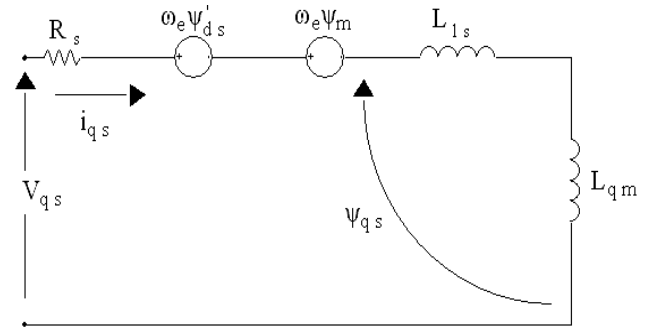


Fig. 3. IPMSM q axis equivalent circuit.

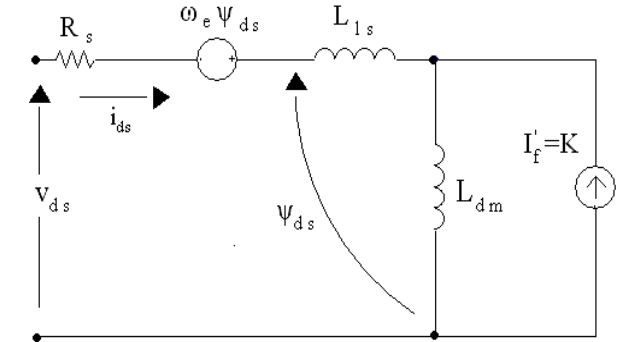


Fig. 4. IPMSM d axis equivalent circuit.

Considering transient equivalent circuits that are given in Fig. 3 and Fig. 4 transient equations of motor are obtained as in (5)–(11):

$$v_{qs} = R_s i_{qs} + \omega_e \psi'_{ds} + \omega_e \psi_m + \frac{d}{dt} \psi_{qs}, \quad (5)$$

$$v_{ds} = R_s i_{ds} - \omega_e \psi_{qs} + \frac{d}{dt} \psi_{ds}, \quad (6)$$

$$\psi_m = L_{dm} I_f', \quad (7)$$

$$\psi_{ds}' = i_{ds} (L_{ls} + L_{dm}) = i_{ds} L_{ds}, \quad (8)$$

$$\psi_{ds} = \psi_m + \psi_{ds}', \quad (9)$$

$$\psi_{qs} = i_{qs} (L_{ls} + L_{qm}) = i_{qs} L_{qs}, \quad (10)$$

$$T_e = \frac{3}{2} p (\psi_{ds} i_{qs} - \psi_{qs} i_{ds}), \quad (11)$$

where ω_e – rotor electrical speed; L_{dm} – d axis magnetizing inductance; L_{qm} – q axis magnetizing inductance; L_{ls} – leakage inductance; ψ_{ds} – stator d axis flux; ψ_{qs} – stator q axis flux; ψ_m – magnetizing flux.

$$T_e = \frac{3}{2} p (\psi_m i_{qs} - (L_{qs} - L_{ds}) i_{ds} i_{qs}). \quad (12)$$

MTPAC optimizes drive efficiency via minimizing electrical losses. Constant torque curves and maximum torque per ampere trajectories can be seen in Fig. 5.

As can be seen from the figure current expression can be obtained like in (13)

$$i_s = \sqrt{i_{qs}^2 + i_{ds}^2}. \quad (13)$$

When q axis current defines torque polarity, d axis current is always negative and it is not affected by torque polarity. When torque need is high (i.e. starting or acceleration), d axis current provides reluctance torque [17].

Stator current components can be obtained from Fig. 5 as in the expressions below. Torque angle (α) value, that is in these equations, is the angle between I_s and I_{qs} [18], [19]:

$$i_{ds} = -i_s \sin \alpha, \quad (14)$$

$$i_{qs} = i_s \cos \alpha, \quad (15)$$

$$T_e = \frac{3}{2} p [\psi_m i_s \cos \alpha + \frac{1}{2} (L_{qs} - L_{ds}) i_s^2 \sin 2\alpha]. \quad (16)$$

As illustrated in Fig. 5 to produce desired torque value the shortest distance between maximum torque/ampere trajectory and torque curve is used. This provides to obtain desired torque value with the shortest current amplitude. When torque equation is differentiated and the differentiation is made equal to zero, maximum T_e/I_s rate can be obtained. It is seen in (17) differentiation of torque is made equal to zero to obtain the current expressions of maximum torque

$$\frac{dT_e}{d\alpha} = 0. \quad (17)$$

Current components that yield achieving maximum torque value are obtained with the expressions below:

$$i_{ds} = \frac{\psi_m - \sqrt{\psi_m^2 + 8(L_{qs} - L_{ds})^2 i_s^2}}{4(L_{qs} - L_{ds})}, \quad (18)$$

$$i_{qs} = \sqrt{i_s^2 - i_{ds}^2}. \quad (19)$$

Using (18) and (19) in (12) to express d and q axes currents as functions of torque, results with nonlinear equations. Solving this equation is rather difficult. On the other hand, curve fitting can also be used to determine the relationship between torque and current.

d and q axes currents should be obtained as functions of torque. However, acquisition of these currents with keeping only torque parameter in i_d and i_q expressions causes rather difficult expressions to form in controller coding. Therefore, relationship between i_s and T_e is obtained with curve fitting. Curve fitting result can be seen in Fig. 6.

Obtained relationship's mathematical expression is given below

$$|i_s|(T_e) = 2.2214T_e + 0.0313. \quad (20)$$

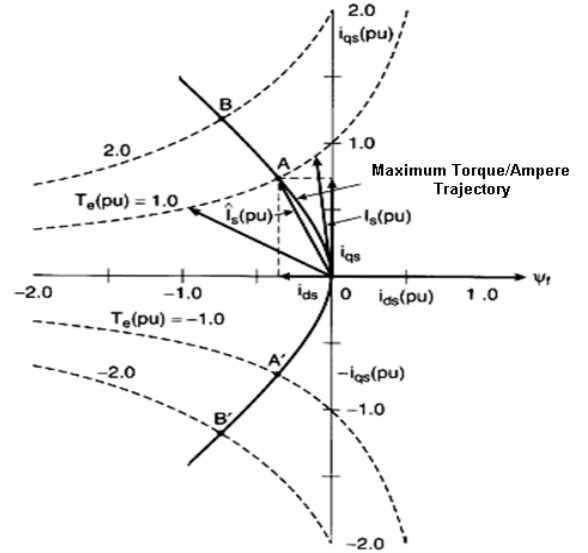


Fig. 5. Constant torque trajectories and MTPA loci.

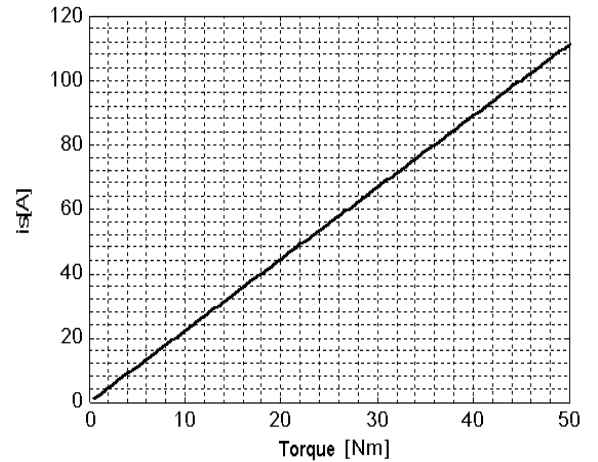


Fig. 6. Torque-current relationship via curve fitting.

When (20) is used in (18) and (19), d and q axes currents expressions are obtained. MTPAC block that can be seen in Fig. 7 gives d and q axes currents which are obtained with curve fitting.

Working in field weakening region makes stator current branch from maximum torque/ampere trajectory because higher negative i_{ds} current is needed to lower the magnet flux. In accordance with (19) when i_{ds} current is heightened to lower the magnet flux in field weakening region, i_{qs} current is suppressed to ensure current limit requirement.

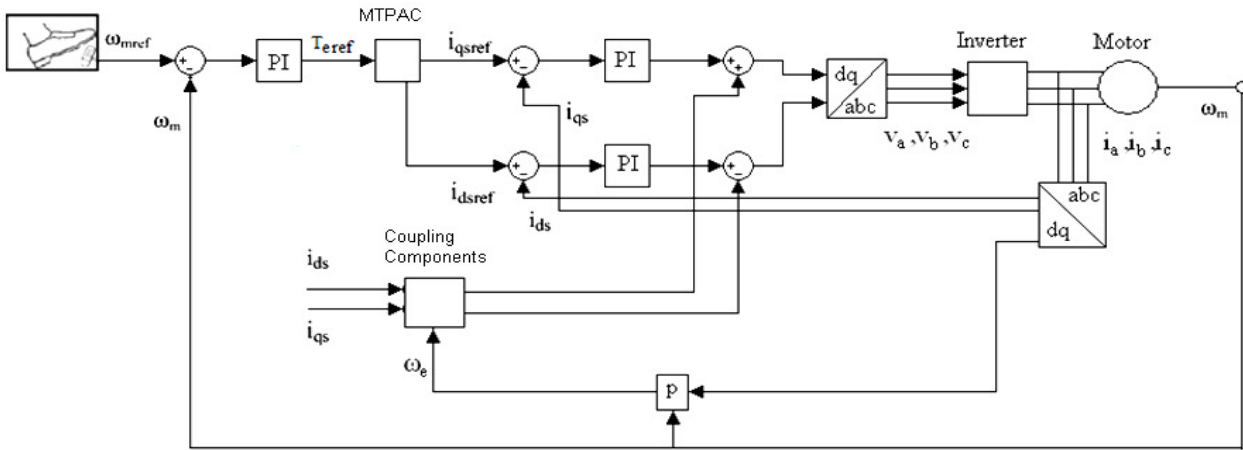


Fig. 7. Block diagram of simulated drive circuit.

IV. SIMULATION RESULTS

In this study an electric vehicle that uses IPMSM as a traction motor simulated with proposed MTPAC method. Nominal values are given below:

- Power: 2.2kW;
- Pole Num.: 2;
- Phase Num.: 3;
- L_d : 6.324 μ H;
- L_q : 10.1 μ H;
- R_s : 9.34 m Ω ;
- ψ_m : 9.9 mWb.

Simulated system's block diagram is given in Fig. 7. In this system speed reference and speed feedback is compared, and torque reference is produced via a PI controller.

Current references of d and q axes are produced via current expressions that obtained with curve fitting. Voltage references are produced from current faults and coupling components. As can be seen from (5) and (6) each axis voltage expression has other axis' components as coupling components. Voltage references are subjected dq-abc conversion and energy is transferred to motor via inverter with space vector modulation. "p" block, which is represented in the block diagram, refers the pole pair number.

System is simulated for both no load operation and full load operation. Base speed is 68.75 rad/s, base torque is 32 Nm. Motor current is used for only overcoming inertia and friction torque in no load operation, and in this operation after overcoming the inertia d axis current becomes zero.

Speed, torque and currents for no load operation can be seen in Fig. 8–Fig. 11. Speed and torque values are given in per unit. On the other hand, while the motor is working with nominal load or full load, torque and current values are differ from no loads. The system utilizes both d and q axes currents to produce maximum torque with the lowest possible current value under full load with the help of reluctance torque. Torque and current values for full load operation can be seen in Fig. 12–Fig. 15. As can be seen from simulation results d and q axes currents obtained via curve fitting are very close to optimum current values that can be obtained via calculation with an acceptable error.

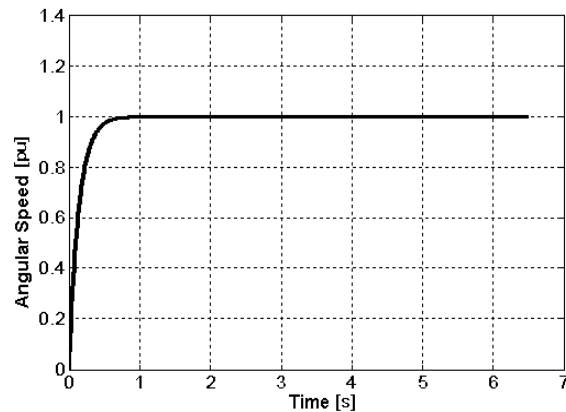


Fig. 8. Angular speed of motor under no-load.

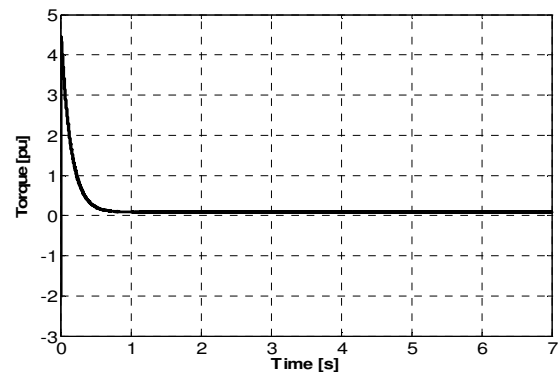


Fig. 9. Electromagnetic torque of motor under no-load.

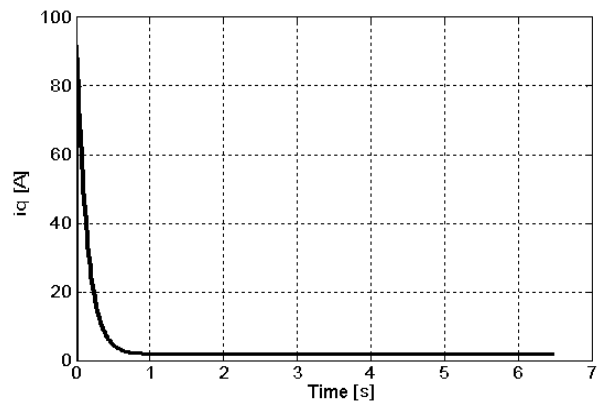


Fig. 10. q axis current of motor under no-load.

Thereby while the controller is achieving its main duty, it operates without difficult calculation processes, so fault possibility is reduced to minimum and performance of controller is highly increased as well as total system performance.

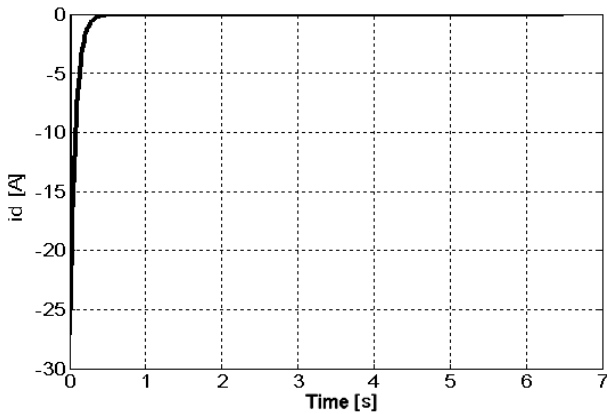


Fig. 11. d axis current of motor under no-load.

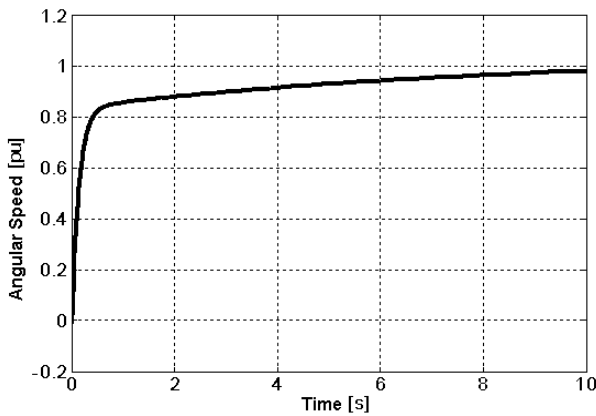


Fig. 12. Angular speed of motor under full-load.

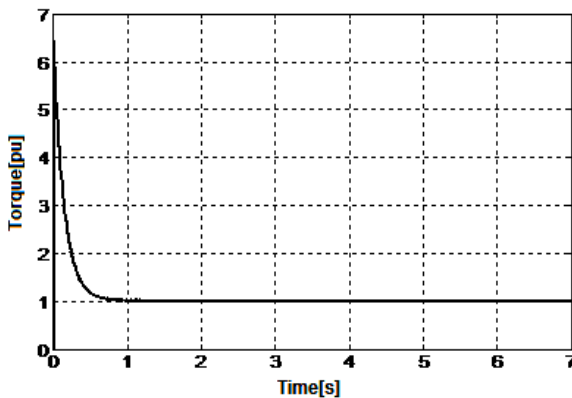


Fig. 13. Electromagnetic torque of motor under full-load.

Nominal speed reference is applied to motor in both no load and full load operations. Motor is produced a torque for only overcoming the friction under no load, and both d and q axes currents are used for overcoming the inertia; on the other hand, in full load operation d and q axes currents are used both in transient operation and steady state operation for optimum current usage that aimed in MTPAC. Due to minimum current requirement for reference torque value efficiency is increased via reducing the losses. Nominal phase currents can be seen in Fig. 16.

On the other hand, while the vehicle is climbing down motor operates in regenerative mode with a negative torque value and, both d and q axes currents become negative to deliver energy back to source.

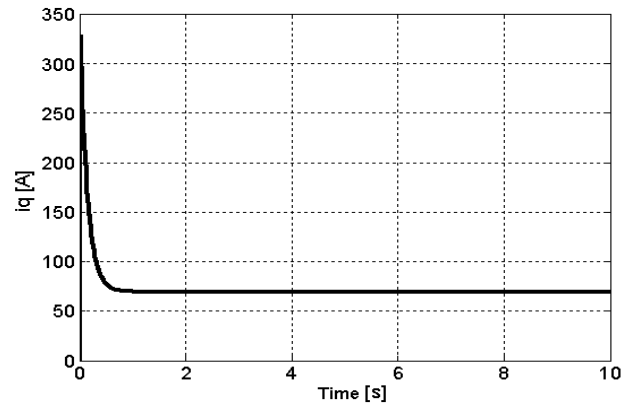


Fig. 14. q axis current of motor under full-load.

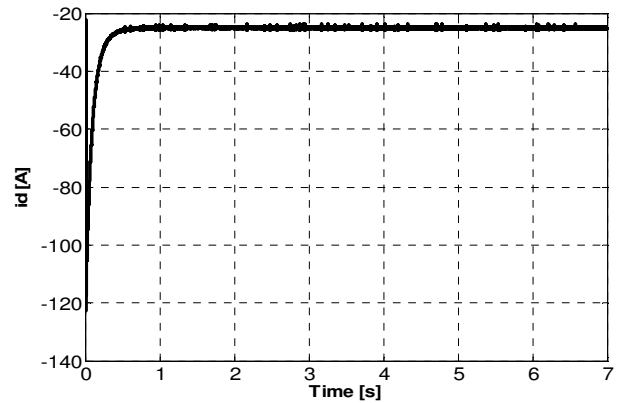


Fig. 15. d axis current of motor under full-load.

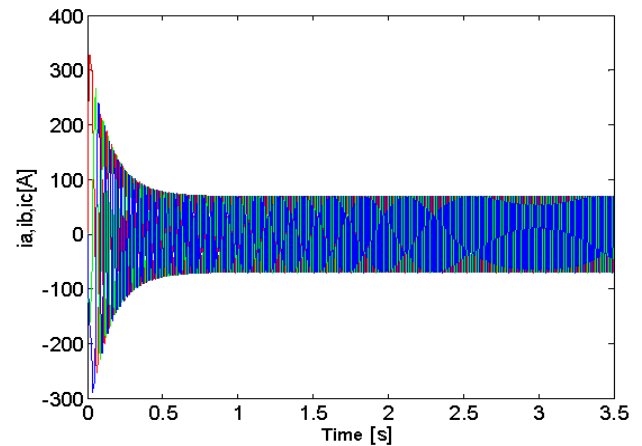


Fig. 16. Motor phase currents under nominal load.

It can be seen from the figures that the results with proposed method are compatible with the nonlinear model of IPMSM, and this demonstrates the effectiveness of proposed method.

V. CONCLUSIONS

In this study a high performance MTPAC drive system for IPMSM used in electrical vehicles is proposed. In the proposed control method nonlinear expression that gives torque-current relationship is converted to a first order linear equation. Thus, optimum current utilization is achieved, and

controller calculation burden is lowered. Consequently, real time performance and reliability is boosted.

It has been seen from the simulation results that in full load conditions both current components are used with the most effective way for producing torque. Reluctance torque is fully utilized. Losses are reduced with this control method due to minimum current requirement, and efficiency is increased. It is shown that proposed method gives compatible results with the nonlinear equations of IPMSM model. As can be seen from the results, MTPAC is one of the most appropriate control methods for IPMSMs, and with the proposed method MTPAC is very simple and suitable for vehicular drive applications.

REFERENCES

- [1] Z. B. Jun, J. Lee, T. Lee, C. Won, "Control of IPMSM for Hybrid Electric Commercial Vehicle", in *Proc. of Vehicle Power and Propulsion Conference*, 2010, pp. 1–4.
- [2] Y. Yi, D. M. Vilathgamuwa, M. A. Rahman, "Implementation of an artificial neural network based real time adaptive controller for an interior permanent magnet motor drive", *IEEE Trans. on Industry Applications*, vol. 39, pp. 96 – 104, 2003. [Online]. Available: <http://dx.doi.org/10.1109/TIA.2002.807233>
- [3] M. A. Rahman, D. M. Vilathgamuwa, M. N. Uddin, K. J. Tseng, "Nonlinear control of interior permanent magnet synchronous motor", *IEEE Trans. on Industry Applications*, vol. 39, pp. 408–416, 2003. [Online]. Available: <http://dx.doi.org/10.1109/TIA.2003.808932>
- [4] M. F. Moussa, A. Helal, Y. Gaber, H. A. Youssef, "Unity power factor control of permanent magnet motor drive system", in *Proc. of Power System Conference*, 2008, pp. 360–367.
- [5] C. Mademlis, N. Margaritis, "Loss minimization in vector controlled interior permanent magnet synchronous motor drives", *IEEE Trans. on Ind. Electronics*, vol. 49, pp. 1344–1347, 2002. [Online]. Available: <http://dx.doi.org/10.1109/TIE.2002.804990>
- [6] S. Huang, Z. Chen, H. Keyuan, J. Gao, "Maximum Torque Per Ampere and Flux-weakening Control for PMSM based on Curve Fitting", in *Proc. of Vehicle Power and Propulsion Conference*, 2010, pp. 1–5.
- [7] Y. P. Xu, Y. R. Zhong, "Simulation of minimum loss control for PMSM", *Journal of System Simulation*, vol. 19, pp. 5283–5286, 2007.
- [8] S. Bolognani, R. Petrella, A. Prearo, L. Sgarbossa, "Automatic tracking of MTPA trajectory in IPM motor drives based on AC current injection", in *Proc. of Energy Conversion Congress and Exposition*, 2004, pp. 2340–2346.
- [9] A. Consoli, G. Scarcella, G. Scelba, A. Testa, "Steady-state and transient operation of IPMSMs under maximum torque per ampere control", *IEEE Trans. on Industry Applications*, vol. 46, pp.121–129, 2010. [Online]. Available: <http://dx.doi.org/10.1109/TIA.2009.2036665>
- [10] D. Lucache, V. Horga, M. Ratoi, A. Simion, M. Albu, "Motoring regime control of an interior permanent magnet synchronous machine", in *Proc. of International Conference on Electromechanical and Power Systems*, Moldova, 2007, pp. 217–222.
- [11] F. Tahami, H. Nademi, M. Razei, "Maximum Torque per Ampere Control of Permanent Magnet Synchronous Motor Using Genetic Algorithm", *Telkomnika*, vol. 9, no. 2, pp. 237–244, 2011.
- [12] M. Ehsani, Y. Gao, S. E. Gay, A. Emadi, *Modern Electric, Hybrid Electric and Fuel Cell Vehicles*. CRC Press, New York, 2005, Ch. 6.
- [13] M. Zeraoulia, M. E. H. Benbouzid, D Diallo, "Electric motor drive selection issues for HEV propulsion systems: a comparative study", *IEEE Transactions on Vehicular Technology*, vol. 55, no. 6, pp. 1756–1764, 2006. [Online]. Available: <http://dx.doi.org/10.1109/TVT.2006.878719>
- [14] C.C. Chan, "The state of the art of electric, hybrid and fuel cell vehicles", in *Proc. of the IEEE*, vol. 95, no. 4, 2007, pp. 704–718. [Online]. Available: <http://dx.doi.org/10.1109/JPROC.2007.892489>
- [15] I. Husain, *Electric and Hybrid Vehicles Design Fundamentals*. CRC press, New York, 2003, Ch. 8.
- [16] G. Bal, *Ozel Elektrik Makinalari*. Seckin Press, Ankara, 2006, Ch. 6.
- [17] V. Erginer, "Electric Vehicles and Drive Circuits", M.S. thesis, Dept. Electrical Eng., Ch. 8, Yildiz Technical University, Istanbul, Turkey, 2009.
- [18] B. K. Bose, *Modern Power Electronics and AC Drives*. Prentice Hall, New Jersey, 2002, Ch. 9.
- [19] B. K. Bose, "A high performance inverter-fed drive system of an interior permanent magnet synchronous machine", *IEEE Transactions on Industrial Applications*, vol. 24, no. 6, pp. 987–997, 1988. [Online]. Available: <http://dx.doi.org/10.1109/28.17470>